Adsorption isotherms and kinetics of activated carbons produced from coals of different ranks

B. Purevsuren, Chin-Jung Lin, Y. Davaajav, A. Ariunaa, S. Batbileg, B. Avid, S. Jargalmaa, Yu Huang and Sofia Ya-Hsuan Liou

ABSTRACT

Activated carbons (ACs) from six coals, ranging from low-rank lignite brown coal to high-rank stone coal, were utilized as adsorbents to remove basic methylene blue (MB) from an aqueous solution. The surface properties of the obtained ACs were characterized via thermal analysis, N_2 isothermal sorption, scanning electron microscopy, Fourier transform infrared spectroscopy, X-ray photoelectron spectroscopy and Boehm titration. As coal rank decreased, an increase in the heterogeneity of the pore structures and abundance of oxygen-containing functional groups increased MB coverage on its surface. The equilibrium data fitted well with the Langmuir model, and adsorption capacity of MB ranged from 51.8 to 344.8 mg g^{-1}. Good correlation coefficients were obtained using the intra-particle diffusion model, indicating that the adsorption of MB onto ACs is diffusion controlled. The values of the effective diffusion coefficient ranged from 0.61×10^{-10} to 7.1×10^{-10} m^2 s^{-1}, indicating that ACs from lower-rank coals have higher effective diffusivities. Among all the ACs obtained from selected coals, the AC from low-rank lignite brown coal was the most effective in removing MB from an aqueous solution.

Key words | activated carbon, adsorption, coal rank, methylene blue

B. Purevsuren
Y. Davaajav
A. Ariunaa
S. Batbileg
B. Avid
S. Jargalmaa
Institute of Chemistry and Chemical Technology,
Mongolian Academy of Sciences,
Ulaanbaatar,
Mongolia

Chin-Jung Lin
Yu Huang
Department of Environmental Engineering,
National Ilan University,
1, Sec. 1, Shen-Lung Road,
I-Lan,
260,
Taiwan

Sofia Ya-Hsuan Liou (corresponding author)
Department of Geosciences,
National Taiwan University,
P.O. Box 13-318,
Taipei 106,
Taiwan
E-mail: *yhliou@ntu.edu.tw*

INTRODUCTION

Dyes are widely used with the rapid development of surface coating and printing industries, such as in pulp mills, dye synthesis, and textile, leather, and wax printing (Crini 2008). The removal of dyes from wastewater has received considerable attention because the majority of organic dyes are harmful to human beings and toxic to microorganisms. Methylene blue (MB), a water-soluble cationic dye mainly used on cotton, wool, and silk, can be hazardous if inhaled in large doses (Ioannou *et al.* 2013). Various MB-removal methods, such as chemical oxidation (Ma *et al.* 2004), coagulation/flocculation (Shi *et al.* 2007), separation (Zaghbani *et al.* 2007), nano-zerovalent iron (Arabi & Sohrabi 2014), biological treatments (Fu & Viraraghavan 2001), and adsorption techniques (Liu *et al.* 2013), have been developed. However, these physico-chemical techniques are limited by complicated equipment, costly operation, and the generation of hazardous intermediates.

Dye adsorption on various adsorbent surfaces is considered a promising method to remove dyes from waste effluents because it is low-cost, flexible, simple in terms of design, easily operated, and insensitive to toxic pollutants. Several kinds of solid adsorbents, such as kaolinite, activated carbon (AC) (Liu *et al.* 2013), agricultural waste (Hameed & Ahmad 2009), are able to efficiently remove dyes from water via physical or/and chemical bonding. ACs, because of their well developed pore structure, large surface area and relatively high adsorption capacity for a wide variety of dyes, have become the most promising and effectively adsorbents in dye removal (Liu *et al.* 2013). However, commercially available ACs are composed of a variety of carbonaceous-rich materials and are expensive; thus, the use of cheap substitutes is being determined.

Bituminous coal-based ACs have been generated in previous studies (Moreno-Castilla *et al.* 1995) to remove dyes from aqueous solutions. The development of an internal pore structure, which consists of micro-, meso-, and macropores, and the number of functional groups on the surface of the ACs are highly dependent on the nature of precursors

doi: 10.2166/wst.2015.094

(Okman *et al.* 2014). The origin of the precursor has a strong impact on the porous texture of ACs and their surface chemistry which govern the adsorption capacity. Here, we fabricated ACs from six coals of different ranks (lignite, bituminous coal, two types of stone coal, high-rank stone coal, and coking coal) in Mongolia and then the surface properties were characterized. Their adsorption equilibrium, isotherms and kinetics were established. The results show that the surface chemistry and the evolution of pore structure were found to be highly dependent on the raw coal type and rank. As coal rank decreased, an increase in the heterogeneity of the pore structures and abundance of oxygen-containing functional groups increased MB coverage on its surface.

MATERIALS AND METHODS

The coal samples were obtained from the six deposits in Mongolia. Table 1 shows the basic coal sample information. The surface properties of the obtained ACs were characterized via thermal analysis, N_2 isothermal sorption, scanning electron microscopy (SEM), Fourier transform infrared spectroscopy (FTIR), X-ray photoelectron spectroscopy (XPS), and Boehm titration (Boehm 1994). For the batch adsorption studies, appropriate AC was added to a series of flasks filled with MB. The adsorption equilibrium, isotherms and kinetics of the ACs from six coals of different ranks were established. All the detailed information is described in the Supplementary Material (available online at http://www.iwaponline.com/wst/071/094.pdf).

RESULTS AND DISCUSSION

Characterization of prepared ACs

Table 1 shows the proximate analysis results of the six coal samples. Volatile matter, carbon and ash contents in coals varied according to coal ranks. The ACs differed obviously in terms of surface area, pore volume, and surface functional groups. The AC with the smallest BET (Brunauer–Emmett–Teller) surface area of 176 $m^2 g^{-1}$ originated from the Tavantolgoi deposits (AC-VI). The AC with the relative larger BET surface area are 508 $m^2 g^{-1}$ and 511 $m^2 g^{-1}$ obtained from the Baganuur (AC-I) and Shariin deposits (AC-II). ACs obtained from low-rank coals, such as AC-I, AC-II, AC-III, and AC-IV, have well developed mesoporous structures. The mesopore contributed to the total surface area are 54%, 41%, 30%, and 30% for AC-I, AC-II, AC-III, and AC-IV while 22% and 15% for AC-V, and AC-VI, respectively. The

Table 1 | Characteristics of the coals and ACs used

	Specifications	AC-I	AC-II	AC-III	AC-IV	AC-V	AC-VI
	Deposit location	*Baganuur*	*Shariin*	*Ereen*	*Nariinsukhait*	*Saikhaovoo*	*Tavantolgoi*
	Coal type	Lignite	Stone coal	Stone coal	Bituminous coal	High-rank stone coal	Coking coal
	Proximate analysis (wt.%, dry base)						
	Volatile matter	11.7	8.4	12.8	6.1	5.7	7.7
	Ash	15.4	13.7	9.6	11.7	6.3	8.0
	Fixed carbon	72.9	77.9	77.6	82.2	88.0	84.3
	Ultimate analysis (wt.%)						
Coals	Carbon	58.4	63.2	68.9	68.6	80.0	83.4
	Hydrogen	4.7	5.5	4.9	4.3	2.0	4.5
	Nitrogen	0.7	1.4	1.4	0.9	1.6	2.3
	Sulfur	0.3	0.2	0.1	0.8	0.2	0.5
	Oxygen	19.8	13.9	12.3	9.1	6.8	5.4
	Acid (meq g^{-1})	0.317	0.323	0.168	0.202	0.188	0.129
	Basic (meq g^{-1})	0.815	0.560	0.630	0.429	0.497	0.517
ACs	Surface area ($m^2 g^{-1}$)[a]	508/223/275	511/305/208	476/332/144	442/310/132	263/204/58	176/149/27
	Pore volume ($cm^3 g^{-1}$)	0.432	0.385	0.297	0.235	0.125	0.119
	Pore size (nm)	6.58	4.52	5.48	4.51	2.07	1.82

[a]BET surface/ *t*-plot micropore surface/ *t*-plot mesopore surface.

total pore volumes are between 0.119 and 0.432 $cm^3 g^{-1}$ and the average pore size are from 1.82 to 6.58 nm. The evolution of the pore structure within the AC is highly dependent on coal rank. Previous results (Tellez-Juárez *et al.* 2014) showed that porosity development depends on ash and volatile matter contents. During pyrolysis/activation of coal, mineral matter catalytically accelerates the gasification reaction and the release of volatile matter are advantageous to develop the porosity. The effects of coal rank on the total surface area, micropore/mesopore surface area, and pore size of ACs are evident. Analysis of the data presented in Table 1 shows that the number of basic sites exceeded that of acidic sites in the prepared samples. Figure 1((a)–(d)) shows the SEM images of AC-I, AC-II, AC-III, and AC-IV, in which the thick wall opened and a wider porosity is created, thus the external surfaces of ACs are full of cavities. Pores of different sizes and shapes could be observed. The surfaces of the AC-V and AC-VI (Figure 1(e) and 1(f)) are the smoother among the samples because of incomplete activation. Lillo-Ródenas *et al.* (2007) found the activation reaction began at higher temperatures as rank coal increased. The incomplete activation may be attributed to its high coal rank, which results in the development of a poor pore structure and a low surface area.

Results for the FTIR spectra of the prepared ACs are given in Figure 2. The spectra for all the samples show some marked similarities, suggesting that they could possess similar functional groups on their surfaces. The broad and flat band at about 3,400 cm^{-1} is assigned to carboxylic group O–H

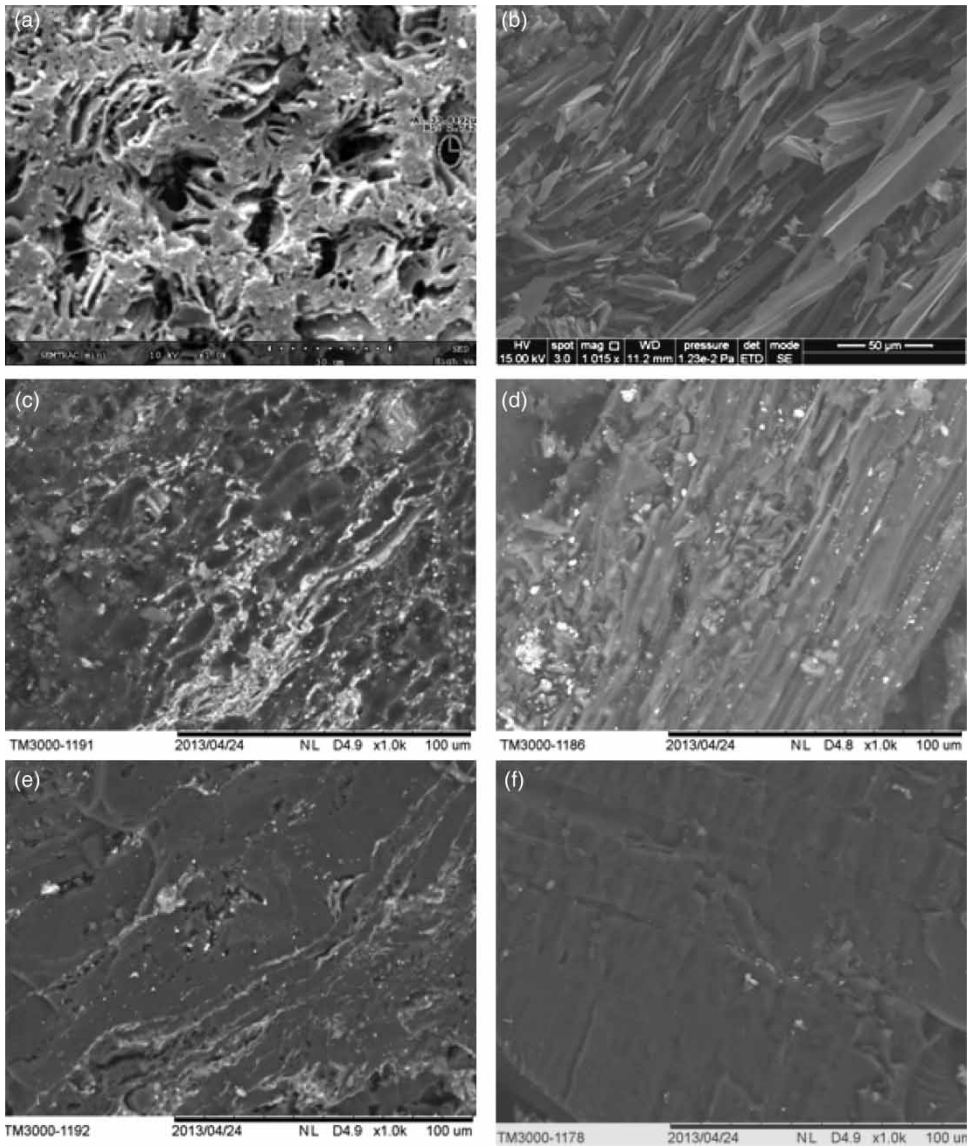

Figure 1 | SEM images of the prepared ACs: (a) AC-I; (b) AC-II; (c) AC-III; (d) AC-IV; (e) AC-V; (f) AC-VI.

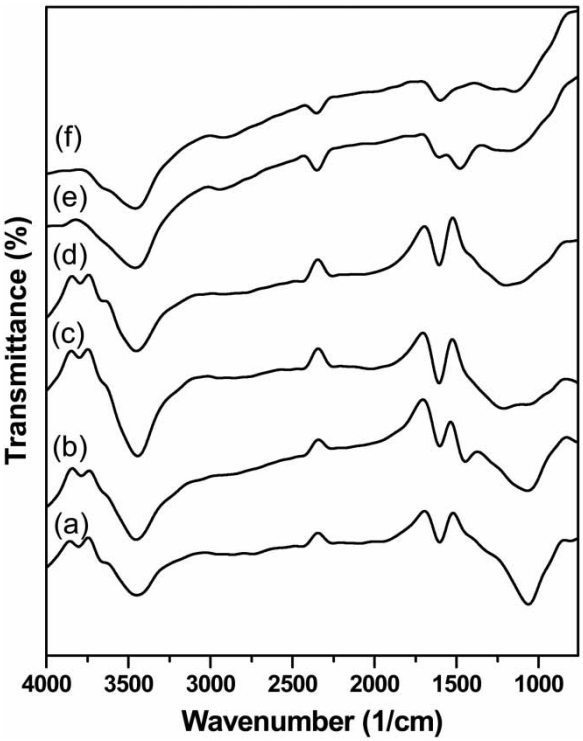

Figure 2 | FTIR spectra of the prepared ACs: (a) AC-I; (b) AC-II; (c) AC-III; (d) AC-IV; (e) AC-V; (f) AC-VI.

stretching (Chen & Wu 2004). Another strong band at 1,750 cm^{-1} is ascribed to CO vibrations probably from esters, ketones or aliphatic acids. The band at 1,620 cm^{-1} can be ascribed to C—C aromatic ring stretching vibration. The peak at 1,245–1,155 cm^{-1} may be assigned to ether, epoxide and phenolic structures in various chemical environments. The band at 1,020 cm^{-1} represents CO stretching vibrations. The peaks are more pronounced in AC-I and AC-II and this would imply the presence of more –CO groups from increased alcohols or ethers than in the other samples. The weaker bands between 765 and 530 cm^{-1} are ascribed to aromatic structures. This clearly indicates that the fabrication process of ACs affected the functional groups according to the coal rank. The XPS spectra of the AC-II show two peaks corresponding to carbon and oxygen in the material (Figure 3). The high resolution O1s spectra (Figure 3(a)) for the AC-II show four peaks corresponding to C═O groups (peak 1, 531.1 eV), C—OH and/or C—O—C groups (peak 2, 532.3 eV), C—O—C═O groups (peak 3, 533.4 eV) and chemisorbed water (peak 4, 535.9 eV). The C1s signals exhibited an asymmetric tailing, which was possibly attributed to the asymmetric of the graphite or oxygen surface complexes (Ma *et al.* 2014). Deconvolution of the C1s spectra gives five individual component peaks (Figure 3(b)), representing carbidic carbon

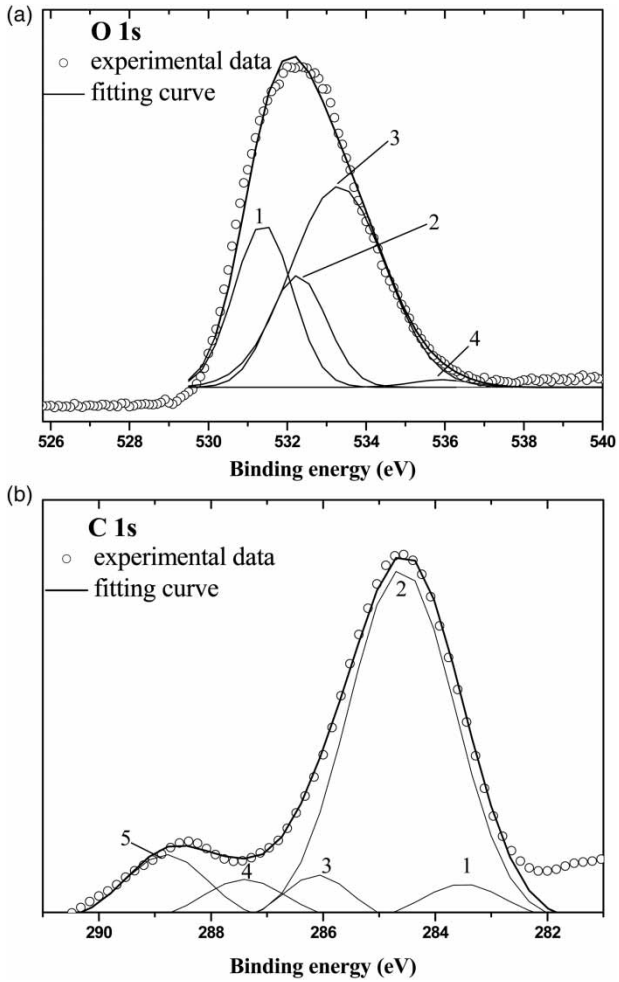

Figure 3 | (a) XP O1s core level spectra of the AC-I materials: (1) C=O; (2) C–OH, C–O–C; (3) C–O–C=O; (4) chemisorbed water, (b) XP C1s core level spectra of the carbon materials: (1) carbidic; (2) graphitic; (3) C–OH, C–O–C; (4) C=O; (5) C–O–C=O.

(peak 1, 283.5 eV), graphitic carbon (peak 2, 284.6 eV), carbon present in alcohol or ether groups (peak 3, 285.8 eV), carbonyl groups (peak 4, 287.4 eV) and carboxyl or ester groups (peak 5, 289 eV). Table S1 in the Supplementary Material (available online at http://www.iwaponline.com/wst/071/094.pdf) summarized the elemental compositions on the surface of AC-I. From the C1s peaks, the oxygen-containing components account for 23.2% of the total C1s intensity (5.9% C—OH; 6.7% C═O and 10.6% C—O—C═O) which means 23.2% of the C atoms on the surface form bonds with O atoms. These results are in agreement with those obtained from the O1s spectra and the O/C ratio being about 20%. The presence of a significant number of carbon-oxygen functional groups on the surface of the AC-I was revealed using FTIR and XPS measurements. The most abundant oxygen-containing groups were phenolic and carbonyl groups.

Adsorption kinetics

Figure S1 in the Supplementary Material (available online at http://www.iwaponline.com/wst/071/094.pdf) shows the percentage of MB uptake at different contact times. Here we used pseudo first-order, pseudo second-order, and the intra-particle diffusion model for describing the adsorption process. The pseudo first-order equation is given by

$$\frac{dq_t}{dt} = k_1(q_e - q_t) \quad (1)$$

where k_1 (h^{-1}) is the equilibrium rate constant of Equation (1). The rate constant, predicted MB uptake, and the corresponding correlation coefficient are listed in Table 2. For the pseudo first-order model, the MB uptakes are obviously underestimated and with low corresponding correlation coefficient. Thus, the pseudo first-order kinetic model is inapplicable for this system. The pseudo second-order equation is the following:

$$\frac{dq_t}{dt} = k_2(q_e - q_t)^2 \quad (2)$$

where k_2 ($g\,mg^{-1}\,h^{-1}$) is the equilibrium rate constant of Equation (2). The parameters are summarized in Table 2. With the exception of AC-V, the correlation coefficient and the MB uptakes determined from the pseudo second-order kinetic model are in good agreement with the experimental data. This implies that the adsorption of MB onto the prepared ACs involves complex physical and chemical sorption. The intra-particle diffusion model is the following equation (Aksu 2005):

$$q_t = k_{int}t^{1/2} \quad (3)$$

where k_{int} is the intra-particle diffusion rate constant ($g\,mg^{-1}\,h^{-0.5}$). Figure S2 in the Supplementary Material (available online at http://www.iwaponline.com/wst/071/094.pdf) shows the amount of dye adsorbed versus $t^{1/2}$ for intra-particle transport of MB by AC from different rank coals. Good correlation coefficients were obtained using the intra-particle diffusion model, indicating that the overall adsorption of MB onto ACs is determined by intra-particle diffusion. The k_{int} values are determined by the intra-particle diffusion effects. The k_{int} values in AC-I, AC-II, AC-III, and AC-IV are much larger than those in AC-V and AC-VI, revealing that the pore structure developed well for MB entry into the ACs through intra-particle diffusion as observed by SEM. Skelland (1974) provided the following simplified equation to calculate the effective particle diffusivity:

$$\ln\left[\frac{1}{1 - F^2(t)}\right] = \frac{\pi^2 D_e t}{R_a^2} \quad (4)$$

where $F(t) = q_t/q_e$ is the fractional attainment of equilibrium at time t, D_e is the effective diffusion coefficient ($m^2\,s^{-1}$), and R_a (m) is the radius of the AC particle. The values of the effective diffusion coefficient (shown in Table 3) ranged from 0.61×10^{-10} to $7.1 \times 10^{-10}\,m^2\,s^{-1}$. The development of coal pore structures with varying coal ranks is implicated in the differences in diffusion rate.

Table 2 | Kinetic parameters for the adsorption of MB onto ACs

AC samples	AC-I	AC-II	AC-III	AC-IV	AC-V	AC-VI
Reaction kinetic model						
Pseudo first-order						
k_1 (h^{-1})	0.53	0.57	0.54	0.60	0.40	0.59
q_e ($mg\,g^{-1}$)	196	184	122	125	75.0	33.0
R^2	0.89	0.96	0.95	0.95	0.95	0.97
Pseudo second-order						
k_2 ($g\,mg^{-1}\,h^{-1}$)	6.01	6.12	3.85	2.56	0.73	4.3
q_e ($mg\,g^{-1}$)	190	191	130	132	80.0	43.0
R^2	0.99	0.99	0.98	0.98	0.94	0.97
Intra-particle diffusion						
k_{int} ($g\,mg^{-1}\,h^{-0.5}$)	0.91	1.04	0.73	1.22	0.49	0.16
$D_e \times 10^{10}$ ($m^2\,s^{-1}$)	5.07	7.10	2.03	5.07	0.61	0.91
R^2	0.98	0.99	0.98	0.98	0.99	0.99

Adsorption isotherms

MB adsorption isotherms on ACs is shown in Figure S3 in the Supplementary Material (available online at http://www.iwaponline.com/wst/071/094.pdf). Two models, Langmuir and Freundlich (Equations (5) and (6)) are used in the present study and their applicability is compared

$$\frac{C_e}{q_e} = \frac{1}{bQ} + \frac{C_e}{Q} \quad (5)$$

where Q ($mg\,g^{-1}$) and b (mg^{-1}) are Langmuir constants related to maximum adsorption capacity and energy of adsorption, respectively.

$$q_e = K_F C_e^{1/n} \quad (6)$$

where K_F ($mg\,g^{-1}\,(L\,mg^{-1})^{1/n}$) is the adsorption capacity of the adsorbent and n is an indication of how favored the

Table 3 | Langmuir and Freundlich constants related to the adsorption isotherms of MB by ACs and correlation coefficient

AC samples	AC-I	AC-II	AC-III	AC-IV	AC-V	AC-VI
Isothermal adsorption model						
Langmuir						
Q (mg g^{-1})	344.8	285.7	166.7	151.5	104.2	51.8
b (mg^{-1})	0.40	0.64	0.28	0.14	1.20	0.23
R^2	0.96	0.96	0.99	0.94	0.98	0.96
RMSE	0.135	0.131	0.011	0.139	0.02	0.126
SSE	0.11	0.107	0.009	0.128	0.02	0.112
Freundlich						
$1/n$	0.628	0.169	0.425	0.287	0.36	0.959
k_F (mg g^{-1} (L mg^{-1})$^{1/n}$)	98.7	43.6	46.0	89.1	52.5	7.09
R^2	0.97	0.93	0.98	0.75	0.99	0.95
RMSE	0.15	0.142	0.034	0.191	0.02	0.165
SSE	0.123	0.125	0.027	0.182	0.02	0.158

adsorption process is. The non-linear regression root mean square error (RMSE) and sum of squares error (SSE) have been applied to assess the quality of fitting (see Supplementary Material, available online at http://www.iwaponline.com/wst/071/094.pdf). Table 3 presents the Langmuir and Freundlich isotherm parameters, RMSE and SSE for MB adsorption onto ACs. Among all the ACs, the Langmuir isotherm model exhibits lower RMSE and SSE values than those of the Freundlich isotherm, indicating that the Langmuir isotherm fitted quite well with the experimental data. All of the systems displayed favorable MB adsorption according to the Freundlich isotherm n values at $n > 1$. A comparative study of the adsorption capacity of different types of ACs used for the removal of MB is presented in Table 3. Maximum monolayer adsorption capacity Q of MB onto AC-I was 344.8 mg g^{-1}. From this result, the carbonyl group is dominant on the surface of AC-I which shows a negatively charge in the experimental condition and strong adsorption to cationic MB. It is noted that abundant primitive pores and high volatility of raw coal are advantageous to develop the mesopore and functional groups on the surface. As coal rank decreased, an increase in the heterogeneity of the pore structures and abundance of oxygen-containing functional groups increased MB coverage on its surface.

CONCLUSIONS

The batch adsorption studies suggest that AC prepared from the low-rank lignite brown coal can be employed as a low-cost and effective absorbent for removal of MB from aqueous solution. SEM analysis showed that the development of AC pore structures varied with coal ranks. FTIR and XPS analysis confirmed phenolic and carbonyl groups are dominant on their surface. Good correlation coefficients were obtained using the intra-particle diffusion model. The values of the effective diffusion coefficient ranged from 0.61×10^{-10} to 7.1×10^{-10} m^2 s^{-1}, indicating that ACs from lower rank coals had higher effective diffusivities. The adsorption capacity of the ACs was found to increase with an increase of the proportion of mesopore contribution to their porous texture and the number of basic sites on the surface. Maximum adsorption capacity of 344.8 mg g^{-1} was achieved using AC made from low-rank lignite brown coal. Low-ranked coal seems to be an alternative precursor for commercial AC production for various environmental applications.

ACKNOWLEDGEMENTS

The research described in this paper was financially supported by the Ministry of Science Council, Taiwan and the Ministry of Education, Culture and Sciences, Mongolia, under contract numbers NSC 100-2923-E-197-001-MY3 and 101-2923-M-002-007-MY3.

REFERENCES

Aksu, Z. 2005 Application of biosorption for the removal of organic pollutants: a review. *Process Biochem.* **40** (3–4), 997–1026.

Arabi, S. & Sohrabi, M. R. 2014 Removal of methylene blue, a basic dye, from aqueous solutions using nano-zerovalent iron. *Water Sci. Technol.* **70**, 24–31.

Boehm, H. P. 1994 Some aspects of the surface-chemistry of carbon-blacks and other carbons. *Carbon* **32** (5), 759–769.

Chen, J. P. & Wu, S. 2004 Acid/base-treated carbons: characterization of functional groups and metal adsorption properties. *Langmuir* **20** (6), 2233–2242.

Crini, G. 2008 Kinetic and equilibrium studies on the removal of cationic dyes from aqueous solution by adsorption onto a cyclodextrin polymer. *Dyes Pigm.* **77** (2), 415–426.

Fu, Y. & Viraraghavan, T. 2001 Fungal decolorization of dye wastewaters: a review. *Bioresour. Technol.* **79** (3), 251–262.

Hameed, B. H. & Ahmad, A. A. 2009 Batch adsorption of methylene blue from aqueous solution by garlic peel, an agricultural waste biomass. *J. Hazard. Mater.* **164** (2–3), 870–875.

Ioannou, Z., Karasavvidis, Ch., Dimirkou, A. & Antoniadis, V. 2013 Adsorption of methylene blue and methyl red dyes from aqueous solutions onto modified zeolites. *Water Sci. Technol.* **67**, 1129–1136.

Lillo-Ródenas, M. A., Marco-Lozar, J. P., Cazorla-Amorós, D. & Linares-Solano, A. 2007 Activated carbons prepared by pyrolysis of mixtures of carbon precursor/alkaline hydroxide. *J. Anal. Appl. Pyrolysis* **80**, 166–174.

Liu, Q. S., Zheng, T., Li, N., Wang, P. & Abulikemu, G. 2013 Modification of bamboo-based activated carbon using microwave radiation and its effects on the adsorption of methylene blue. *Appl. Surf. Sci.* **265** (10), 919–924.

Ma, L. M., Ding, Z. G., Gao, T. Y., Zhou, R. F., Xu, W. Y. & Liu, J. 2004 Discoloration of methylene blue and wastewater from a plant by a Fe/Cu bimetallic system. *Chemosphere* **55**, 1207–1212.

Ma, X., Zhang, F., Zhu, J., Yu, L. & Liu, X. 2014 Preparation of highly developed mesoporous activated carbon fiber from liquefied wood using wood charcoal as additive and its adsorption of methylene blue from solution. *Bioresour. Technol.* **164**, 1–6.

Moreno-Castilla, C., Rivera-Utrilla, J., López-Ramón, M. V. & Carrasco-Marín, F. 1995 Adsorption of some substituted phenols on activated carbons from a bituminous coal. *Carbon* **33** (6), 845–851.

Okman, I., Karagöz, S., Tay, T. & Erdem, M. 2014 Activated carbons from grape seeds by chemical activation with potassium carbonate and potassium hydroxide. *Appl. Surf. Sci.* **293**, 138–142.

Shi, B. Y., Li, G. H., Wang, D. S., Feng, C. & Tang, H. 2007 Removal of direct dyes by coagulation: the performance of preformed polymeric aluminum species. *J. Hazard. Mater.* **143** (1–2), 567–574.

Skelland, A. H. P. 1974 *Diffusional mass transfer*. Wiley, NY.

Tellez-Juárez, M. C., Fierro, V., Zhao, W., Fernández-Huerta, N., Izquierdo, M. T., Reguera, E. & Celzarda, A. 2014 Hydrogen storage in activated carbons produced from coals of different ranks: effect of oxygen content. *Int. J. Hydrogen Energy* **39** (10), 4996–5002.

Zaghbani, N., Hafiane, A. & Dhahbi, M. 2007 Separation of methylene blue from aqueous solution by micellar enhanced ultrafiltration. *Separ. Sci. Tech.* **55** (1), 117–124.

First received 19 November 2014; accepted in revised form 11 February 2015. Available online 25 February 2015